Available online at www.sciencedirect.com

ScienceDirect

Energy Procedia 00 (2013) 000–000

Energy Procedia

www.elsevier.com/locate/procedia

GHGT-12

Comment [S1]: Elsevier volume and page numbers.

# Large scale $CO_2$ storage with water production

Dag Wessel-Berg[a], Per Bergmo[a], Alv-Arne Grimstad[a], Jørgen Stausland[b]

[a]*SINTEF Petroleum, S.P.Andersens vei 15b, N-7465 Trondheim, Norway.* [b]*NTNU, 7491 Trondheim, Norway*

**Abstract**

$CO_2$ storage without water production is realized by injecting $CO_2$ into the underground without any actions for relieving the pressure buildup generally associated with such an operation. Successfully storing large volumes of $CO_2$ at a given site with no active pressure relief is not guaranteed due to uncertainty of the size and permeability of the hydraulically connected complex connecting to the gas injectors. With water producers active pressure management is possible, and the volume of produced water liberates corresponding pore volume that is available for storage of $CO_2$ without any pressure buildup. Also the relevant size of the storage complex is mainly confined to the region between the injectors and producers, thus reducing the amount of uncertain geology involved. In this paper we run 144 generic 5-spot well pattern Eclipse simulations to assess the effect of petrophysical and operational input parameters. It is seen that storage efficiency and gas breakthrough times can be relatively sensitive to the input parameters, highlighting some of the challenges when a planning a real large scale $CO_2$ storage project. It is also seen that that the 5-spot storage pattern is quite efficient for gas storage, ranging from 9.7% to 62.5% reservoir volume gas per effective pore volume stored at gas breakthrough in the water producer


Selection and peer-review under responsibility of GHGT.

*Keywords:* $CO_2$ storage, water production, 5-spot

## 1. Introduction

CCS (carbon capture and storage) is considered as one of the important options for curbing the increasing levels of $CO_2$ in the atmosphere. Executing a CCS project obviously requires, apart from capture and transport, sufficient storage space, acceptable or no leakage from the underground, as well as a sufficient gas injection rate into the aquifer. The most uncertain part of the CCS value chain is by far the geology of the proposed deep saline storage site. In particular, without pressure relief from water producer wells, the largely unknown size and permeability of the hydraulically connected region will to a high extent dictate the $CO_2$ storage capacity as pressure is propagated significantly further away from the injection well than the extent of the $CO_2$ plume. Overestimation of the size of this connected region is clearly a possible pitfall, or using a spatial limited simulation model with open boundaries to


Selection and peer-review under responsibility of GHGT.

assess storage capacity will generally lead to a corresponding overestimation of the storage capacity. Optimistic models also underestimate the pressure buildup, thus the predicted risk of pressure induced fracturing of the cap rock might not be appreciated. A number of these issues are not relevant to the same degree when water producers are allowed to relieve the pressure in the underground. In particular, uncertainties about the geology far from the $CO_2$ plume do not have the same relevance, problems with pressure buildup and cap rock fracturing is reduced, and the storage capacity per land area is generally greatly improved. In addition, the possibility of drilling water producers in case of unanticipated pressure buildup would significantly reduce the uncertainty of being able to meet a given injection rate in a CCS project. Also the water producers serve as observation well in addition to relieving the pressure. The introduction of water production wells would increase costs for small scale successful $CO_2$ injection projects such as Sleipner [1]. However, if the required target injection rate is significantly higher, pressure buildup is likely to be a limiting factor for storage capacity, and drilling water production wells would be necessary.

In this paper one has systematically varied input parameters for homogeneous horizontal quarter spot models, allowing one to extrapolate the results to approximate storage capacity of a 5-pot pattern with any number of wells. Apart from types of wells (horizontal/vertical), shapes of saturation functions, and numerical choices, the number of dimensionless groups governing the physics for these homogeneous models is relatively modest. Thus, having made some assumptions, it is possible to explore the parameter input space and investigate sensitivities for storage capacities and gas breakthrough times.

**Nomenclature**

| | |
|---|---|
| $L$ | x- and y-length of model |
| $H$ | height of model |
| $\varphi$ | porosity |
| $k_h, k_v$ | horizontal and vertical permeability |
| $g$ | acceleration of gravity |
| $S_{wrg}$ | residual water saturation after gas flooding |
| $k_{rg}^0, k_{rw}^0$ | endpoint relative permeability values |
| $P_c^*$ | reference capillary pressure value |
| $\rho_{g,std}$ | mass density of $CO_2$ at standard conditions |
| $\Delta\rho$ | mass density difference between water and $CO_2$ |
| $\mu_g, \mu_w$ | viscosities |
| $B_g, B_w$ | volume formation factors |
| $\Delta p$ | bottom hole pressure difference between injector and producer |
| $L_{perf}$ | length of perforated interval for horizontal producer |
| $Q_{g,std}$ | standard volume stored gas at breakthrough |
| $Q_{w,std}$ | standard volume brine produced at breakthrough |
| $c_T$ | total compressibility |

## 2. Assumptions and scaling

One considers a class of 3D homogeneous non-tilted Eclipse simulation models with equal lengths in the x- and y-direction. A vertical $CO_2$ injection well is placed in one corner, perforated in the whole interval, and a horizontal water producer is situated at the bottom in the opposite corner. This configuration models a quarter of a unit with

one central producer and 4 injectors, where ¼ of the streamlines from each injector reaches the producer. Due to symmetry one can then extrapolate the simulation results to large 5-spot well configurations

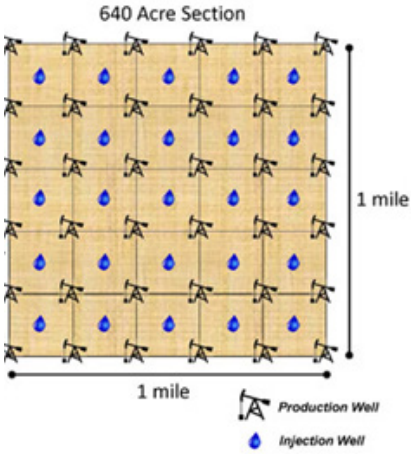


Figure 1 Five spot pattern of injectors and producers. Illustration taken from [2]

Both wells have 10cm diameter. Injection of $CO_2$ and production of water are controlled by bottom hole pressure, and simulations are stopped at gas breakthrough. The amount of injected $CO_2$ is then defined as stored $CO_2$.The producer bottom hole pressure equals the hydrostatic pressure, while the injection pressure is set to two values at each depth, one to 60% of lithostatic pressure, and one with half the pressure drop of that between injector and producer. The lithostatic pressure is assumed to increase by 2.5 bars per 10m. Note that half the length of the perforated interval of the water producer in a full 5-spot pattern is used in the quarter spot model.
Numerical grid blocks are 50mx50mx2m, except for the top 6m of the aquifer, where dz is progressively refined to 0.25m. The relative permeabilities are fixed and are *based on* the values in [3] measured on a Berea core. The measured capillary pressure curve is estimated from [4]. The capillary pressure used in this study has an entry pressure of 0.02 bar, and maximal vale 0.27 bar. The measured core scale relative permeabilities have been used for determining directional dependent (horizontal and vertical) pseudo relative permeabilities. The coarse scale critical gas saturation was estimated to 0.31 and 0.28 in the horizontal and vertical direction respectively, values seeming relatively independent of the flow rates applied in this study. Furthermore, it is assumed that the temperature increases with 3˚C per 100m deeper into in the underground. PVT data for brine and $CO_2$ are then functions of depth and salinity defined by the hydrostatic pressure, the temperature, and the salinity of the brine using the correlations used in [5].With these choices, the following 6 parameters are varied:

- Depth of aquifer (1100m, 2100m)
- Thickness of aquifer (20m, 60m, 120m)
- Vertical permeability (5mD, 100mD, 500mD)
- Brine salinity (4wt%, 20wt%)
- Perforation interval length for horizontal quarter spot water producer (50m, 150m)
- Injection pressure (60% of lithostatic pressure, half delta p)

From a standard scaling analysis of the governing partial differential equations, and with the given assumptions, one is left with 5 independent dimensionless groups defining the parameter input space. These are

Aspect ratio $$\pi_1 = R^2 = \frac{L^2 k_v}{H^2 k_h} \quad (1)$$

Brine/gas end-point mobility ratio $$\pi_2 = M = \frac{k_{rw}^0 \mu_g}{k_{rg}^0 \mu_w} \quad (2)$$

Capillary to viscous force $$\pi_3 = N_{cv} = \frac{P_c^*}{\Delta p} \quad (3)$$

Gravity to viscous force $$\pi_4 = N_{gv} = \frac{\Delta \rho g H}{\Delta p} \quad (4)$$

Perforation interval length to model scale $$\pi_5 = \xi = \frac{L_{perf}}{L} \quad (5)$$

This 5D space of dimensionless parameters is covered by varying the above 6 physical input parameters. In particular, we keep the lengths in the x- and y-direction, $L$, constant to 1500m, and the horizontal permeability equal to 500mD. Let

$$Q_{gD} = \frac{Q_{g,std} B_g}{L^2 H \varphi \left(1 - S_{grw}\right)} \quad (6)$$

be stored reservoir gas volume per effective pore volume, and let

$$Q_{wD} = \frac{Q_{w,std} B_w}{L^2 H \varphi \left(1 - S_{grw}\right)} \quad (7)$$

be produced reservoir volume water per effective pore volume.

$Q_{gD}$ is then one measure of storage capacity. Another, perhaps more appropriate measure for storage capacity would be mass $CO_2$ stored per land area

$$E_{areal} = \frac{Q_{g,std} \rho_{g,std}}{L^2}. \quad (8)$$

Here gas stored at breakthrough is reported using $Q_{gD}$. Note that $Q_{wD}$ is typically a few percent less than $Q_{gD}$, since storage is mainly through exchange of water to gas in the pore space.

Regarding gas breakthrough time, the time scale for 1D Darcy flow of water over length $L$ is

$$T = \frac{L^2 \mu_w \varphi \left(1 - S_{wrg}\right)}{\Delta p k_h k_{rw}^0}, \quad (9)$$

and dimensionless breakthrough time is $t_{btD} = \frac{t_{bt}}{T}$. $t_{btD}$ is then a measure for "early" or "delayed" gas breakthrough in a relative manner. Note that $Q_{gD}, Q_{wD}$, and $t_{btD}$ are functions of $\pi_1, .., \pi_5$. Thus the physical stored and produced standard volumes are given as

$$Q_{i,std} = \frac{L^2 H \varphi \left(1 - S_{grw}\right)}{B_i} Q_{iD}\left(\pi_1, ..., \pi_5\right), \; i = g, w, \quad (10)$$

and the physical breakthrough time

$$t_{bt} = \frac{L^2 \mu_w \varphi \left(1 - S_{wrg}\right)}{\Delta p k_h k_{rw}^0} t_{btD}\left(\pi_1, ..., \pi_5\right). \tag{11}$$

The average standard volume gas injection rate is then

$$\overline{q}_g = \frac{Q_{g,std}}{t_{bt}} = \left(\frac{\Delta p k_h k_{rw}^0 H}{B_g \mu_w}\right) \frac{Q_{gD}\left(\pi_1, ..., \pi_5\right)}{t_{btD}\left(\pi_1, ..., \pi_5\right)}. \tag{12}$$

Here

$$\overline{q}_{gD} = \frac{Q_{gD}}{t_{btD}} \tag{13}$$

is the dimensionless average injection rate.

For $CO_2$ injection *without* water production, let $\Delta\overline{p}$ be the corresponding average pressure increase in the hydraulically connected storage complex having pore volume $V_{por}$. Then the standard volume of gas stored is $V_{por}\Delta\overline{p}c_T$. Thus, for this method of $CO_2$ storage, the fraction of pore space available for gas storage is merely $\Delta\overline{p}c_T$, which typically is less than 1%.

Also note that the typical time scale for pressure propagation over a length $L$ is $\frac{L^2 \varphi \mu_w c_T}{k_h}$, which is of order 10 days for the models considered here (assuming $c_T \approx 10^{-4} bar^{-1}$). Thus the effect of a water producer is felt quite instantaneously in the simulations in the study given in this study.

The proposed models are simple and supposed to represent generic reference cases for understanding better the impact of various input parameters. We disregard the presence of heterogeneity, varying aquifer thickness, gas stored as "attic" gas due to a bumpy cap rock, as well as dipping aquifers. In particular, the existence of thief zones between injector and producer would generally have a significant impact on stored gas volumes and breakthrough times.

**3. Simulations**

A simulation case with a full 5-spot pattern was performed and compared to the corresponding quarter model employed in this study. The difference in stored volume and breakthrough times were acceptable, both less than 2%. To assess needed vertical grid resolution, the top part of the quarter spot simulation grid was progressively refined, and the simulated results (storage and breakthrough time) stabilized well with the values applied for the grid in this study. Also different Corey exponents for the gas and water relative permeabilities were tested. In particular, it is seen that a high gas Corey exponent (=6) significantly increases stored volumes at breakthrough. By testing this case against a case with horizontal Corey exponent equal to 2, and vertical exponent equal to 6, one finds that the effect of improved storage is due to delayed gas segregation improving the gas sweep. However, as discussed, it is chosen to fix the relative permeabilities in the study using measured values and directional pseudo relative permeabilities with critical gas saturations correcting for numerical dispersion. The chosen laboratory capillary pressure curve indeed affects breakthrough times and stored volumes by dispersing the gas front and increasing areal sweep. For some test cases it is indicated that the relatively modest capillary pressure curve used for this study, with entry pressure 0.02 bars and maximal value 0.27 bars, delays breakthrough time and increases storage by typically 20-25%.

Maximal injection pressure is set to 60% of the lithological pressure, and the low injection pressure cases are run with an injection pressure corresponding to half the pressure drop of the maximal.
Water production data is not reported, as they typically are a few percent less than the reservoir gas volume stored.

Generation of the input files for the 144 simulations, execution of the simulations, and post processing of data were automated using UNIX scripts.

Figure 2 shows gas saturation at gas breakthrough for the two cases having lowest and highest storage efficiency, 9.7% and 62.5% of effective pore space respectively. The effective pore space is defined by $L^2 H \varphi \left(1 - S_{wrg}\right)$.
Both cases in Figure 2are for the thickest aquifer with short producer perforation interval. The lowest storage efficiency case has low injection pressure at depth 1000m (dp=35 bars), high salinity (20wt %), and high vertical permeability (500mD). The other case has high injection pressure (dp=108 bars) at depth 2000m, low salinity (4wt %), and importantly, low vertical permeability (5mD).

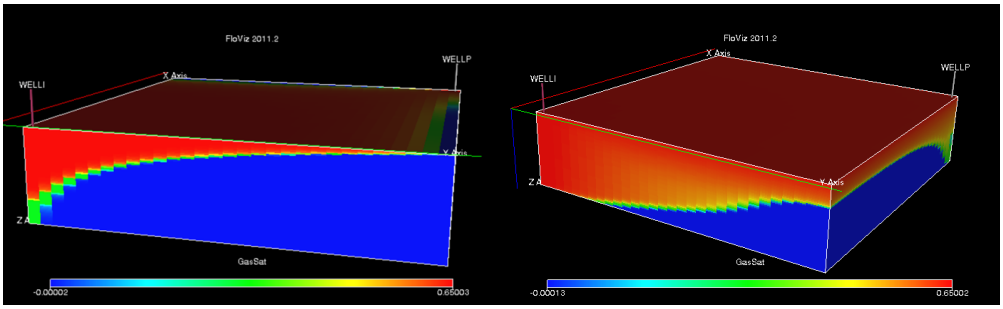


Figure 2 Gas saturation at gas breakthrough for the two cases having lowest and highest storage efficiency, 9.7% and 62.5% of effective pore space respectively.

### *3.1. Results*

Presenting results from the 144 simulations is challenging, and it is chosen to first present physical data for the 20m thick, 1000m deep aquifer, giving stored reservoir volumes of gas per effective pore volume, breakthrough times, and average injection rates. Also data from the deep thick aquifer (120m) with high injection pressure is presented for comparison. Then plots from all cases are presented which indicate the range and distribution of the magnitude of the stored gas for the different cases.

#### *3.1.1. Shallow 20m thick aquifer.*

The first two plots are for different injection pressures, and show stored gas as function of vertical permeability for the different salinities and number of perforations. Each (numerical) perforation corresponds to a perforated interval of 50m.

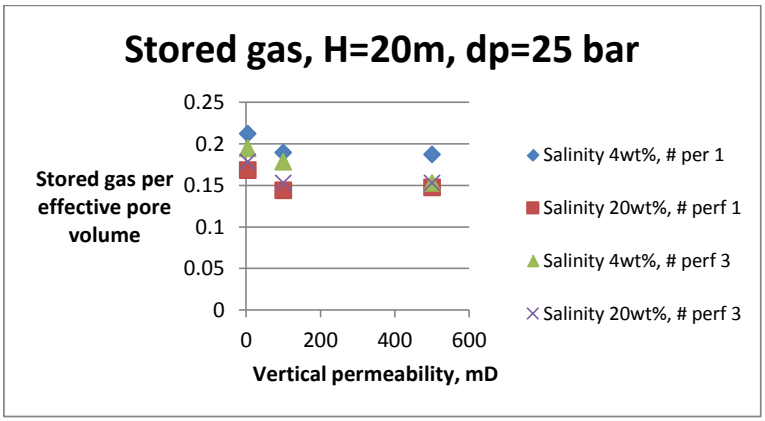


Figure 3 Stored gas per effective pore volume for low injection pressure for thin aquifer and low injection pressure.

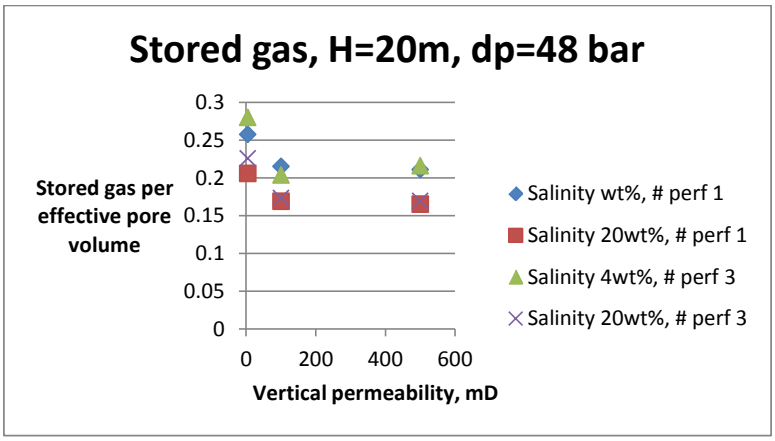


Figure 4 Stored gas per effective pore volume for high injection pressure for thin aquifer with high injection pressure.

From the two plots one observes that increasing the injection pressure increases storage, and that the high salinity cases consequently decrease storage. The increased salinity lowers water mobility, making the gas displacement more unstable, reducing the gas sweep. We also observe that low vertical permeability does not dramatically increase storage for the thin aquifer case. Also the number of perforations does not affect *storage*. From Figure 5 one observes that low vertical permeability is significantly increasing storage for the thick aquifer. Especially, due to the producer position at the bottom, gas breakthrough is significantly delayed with low vertical communication, enhancing storage. The case with maximal storage is the maximal storage case illustrated in Figure 2.

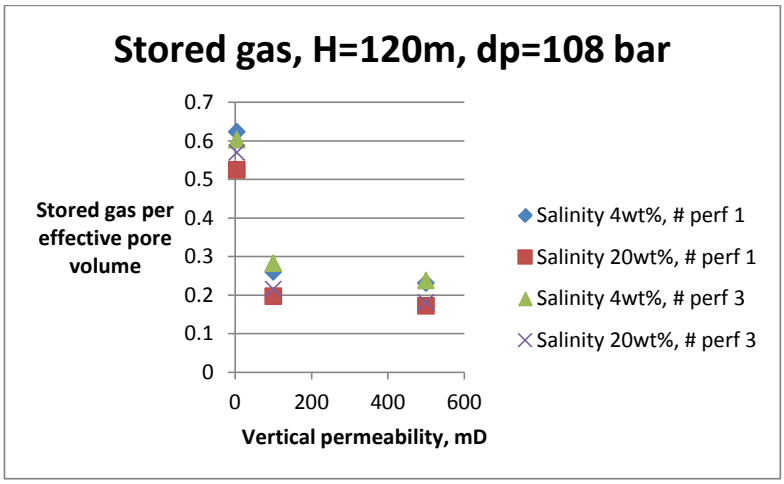


Figure 5 Stored gas per effective pore volume for thick aquifer and high injection pressure.

Even though the storage efficiency for thin aquifers is not significantly affected by vertical permeability, the two figures below illustrate how decreased vertical permeability significantly increases breakthrough time. As expected, one also observes that breakthrough time scales roughly with the pressure drop between injector and producer.

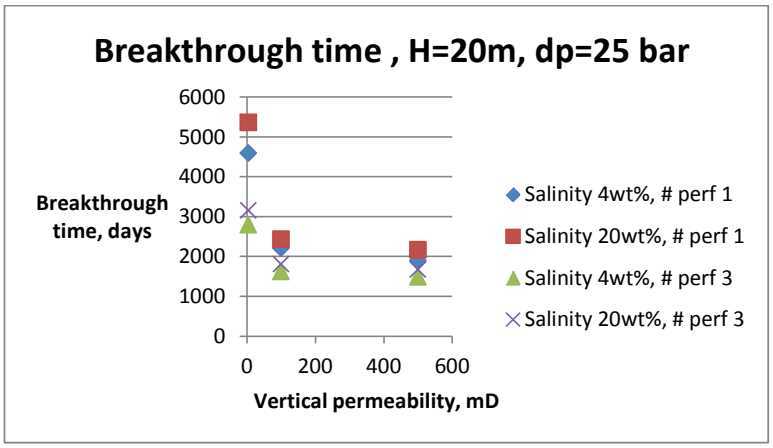


Figure 6 Breakthrough times for thin aquifer and low injection pressure.

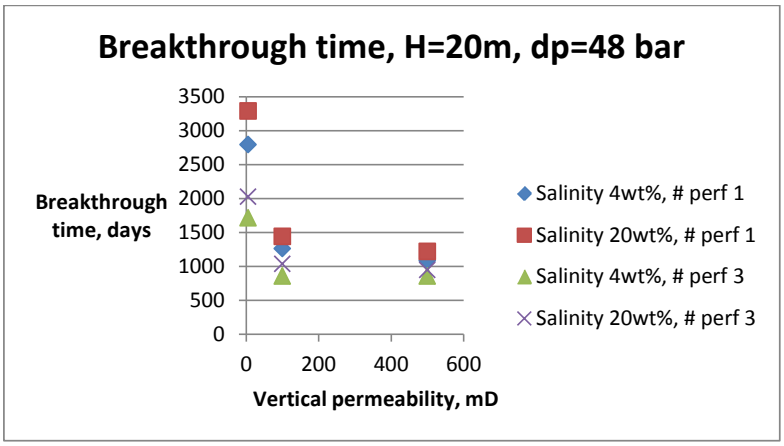


Figure 7 Breakthrough times for thin aquifer and high injection pressure.

The average injection rates are illustrated in Figure 8 and Figure 9, and it is observed that increasing perforation interval length affects injection rate notably, even though this increase does not generally increase storage capacity. Rates increase approximately 30% when extending the perforated interval from 50m to 150m. Note that the reported injection rates are one quarter of what the well would inject in a full 5-spot pattern as only one fourth of the injected gas in such a 5-spot pattern enters the simulation domain. Again one observes that injection rates scale well with the pressure drop between the injector and producer. Furthermore, it is seen that low vertical permeability decreases injection rates, and that rates are relatively sensitive to brine salinity.

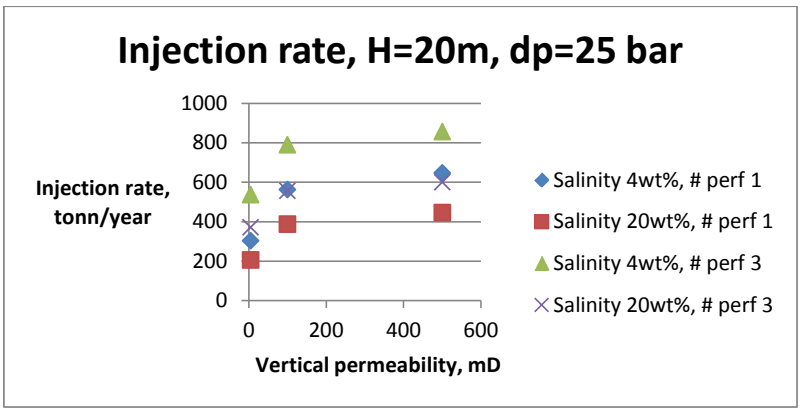


Figure 8 Injection rates times for thin aquifer and low injection pressure.

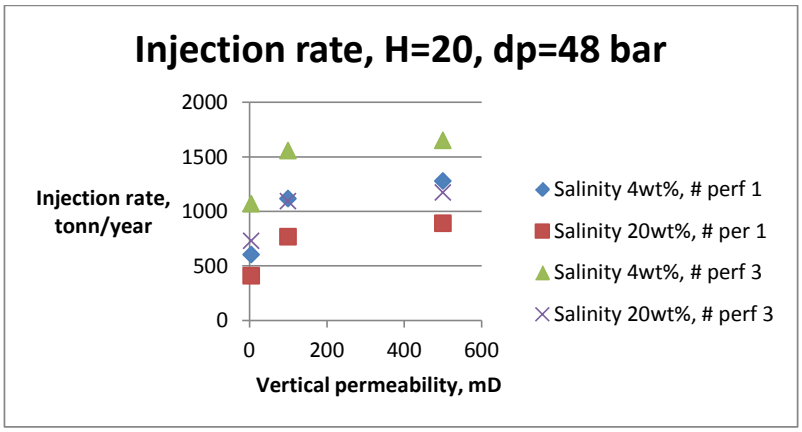


Figure 9 Injection rates times for thin aquifer and high injection pressure.

*3.1.2. All cases*

Next, gas storage efficiency is presented in a manner demonstrating its range for given values of aquifer thickness, vertical permeability, perforation interval length, pressure drop, and salinity. From Figure *10* (a) one observes that the range of storage efficiencies increases with aquifer thickness, and that maximal efficiency increases with aquifer thickness.

From *Figure 10* (b) one sees the range of storage efficiencies is significantly larger for the low vertical permeability. The two other cases have a much more narrow range, indicating that when vertical communication is good, the storage efficiency is not very dependent on the other input parameters.

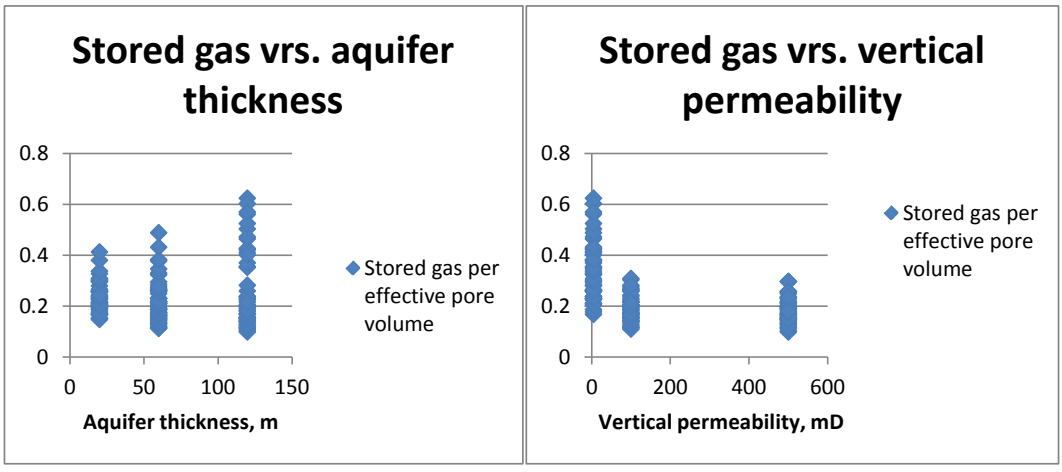


Figure 10 (a) Stored reservoir volumes of gas versus aquifer thickness. (b) Stored reservoir volumes of gas versus vertical permeability.

As seen in Figure 11(a), the ranges for storage efficiency to the two perforation interval lengths, 50m and 150m (which would correspond to horizontal wells in a full 5-spot model with perforated interval lengths of 100m and

300m) are virtually equal and giving the full range of efficiencies. The main effect of increasing perforation interval length is illustrated in Figure 13, showing that injection rates generally increase with increasing perforation length. From Figure 11(b) we observe how increased injection pressure generally increases storage efficiency. It is seen from simulation saturation plots that gas segregates less at increased rates, implying increased storage.

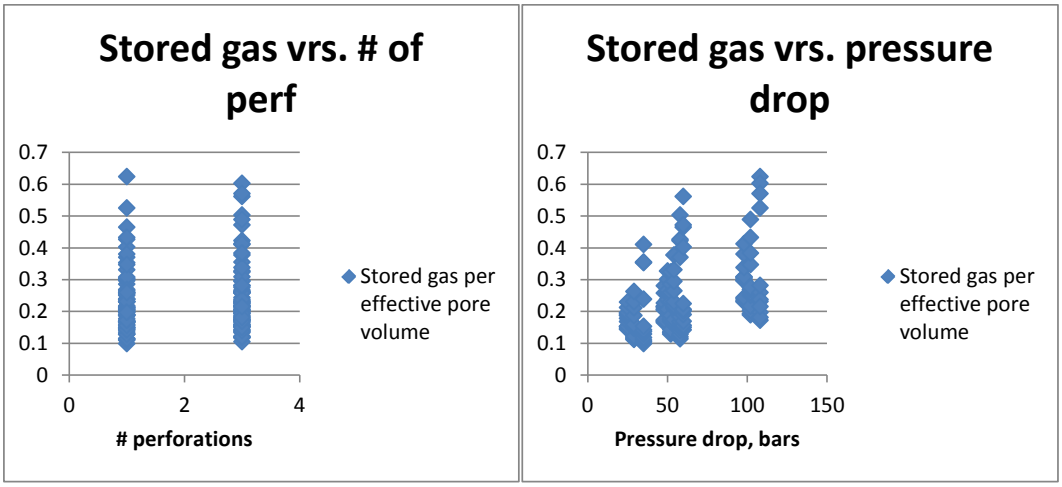


Figure 11 (a) Stored reservoir volumes of gas versus number of perforations. (b) Stored reservoir volumes of gas versus applied pressure drop between injector and producer.

The main effect of increased salinity is the decrease in brine mobility, and from Figure 12 (a) one sees that the high salinity case gives a range of storage efficiencies with lower maximum and minimum compared to the low salinity case.
As discussed, Figure 12 (b) shows how dimensionless injection rate increases with perforation interval length.

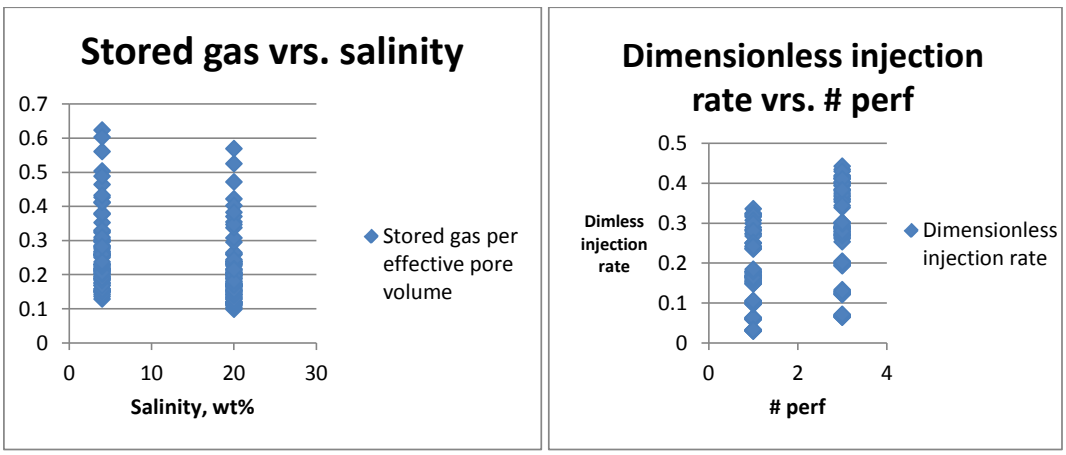


Figure 12 (a) Stored reservoir volumes of gas versus salinity. (b) Dimensionless injection rate versus perforation length.

## 4. Conclusions

- The simulation study suggests that 5-spot pattern storage is a very efficient method for utilizing the underground pore space for $CO_2$ storage.
- For homogeneous models considered here the range of stored reservoir volume of gas per effective pore volume is 9.7% to 62.5%.
- Storage capacity is relatively insensitive to length of the perforated interval of the horizontal water producer. However, injection rates increase notably when increasing this length from 50m to 150m.
- Low vertical communication increases the storage efficiency in general, especially for the thickest aquifer.
- Higher injection pressure increases storage efficiency.
- Higher salinity means less storage efficiency and smaller injection rate.

## Acknowledgements

This publication has been produced with support from the BIGCCS Centre, performed under the Norwegian research program *Centres for Environment-friendly Energy Research (FME)*. The authors acknowledge the following partners for their contributions: ConocoPhillips, Gassco, Shell, Statoil, TOTAL, GDF SUEZ and the Research Council of Norway (193816/S60).

## References

[1] R.A. Chadwick ,D. Noy, R. Arts, O. Eiken. Latest time-lapse seismic data from Sleipner yield new insights into $CO_2$ plume development. Energy Procedia Volume 1, Issue 1, February 2009, Pages 2103–2110.

[2] ] http://www.sec.gov/Archives/edgar/data/8504/000114420413017757/v339500_ex99-1.htm

[3] Samuel C. M. Krevor,Ronny Pini, Lin Zuo, and Sally M. Benson. Relative permeability and trapping of CO2 and water in sandstone rocks at reservoir conditions. WATER RESOURCES RESEARCH, VOL. 48, W02532,doi:10.1029/2011WR010859, 2012

[4] Tetsu K. Tokunaga, Jiamin Wan, Jong-Won Jung, Tae Wook Kim, Yongman Kim, and Wenming Dong. Capillary pressure and saturation relations for supercritical CO2 and brine in sand: High-pressure Pc(Sw) controller/meter measurements and capillary scaling predictions. WATER RESOURCES RESEARCH, VOL. 49, 4566–4579, doi:10.1002/wrcr.20316, 2013

[5] Erik Lindeberg. Calculation of thermodynamic properties of CO2, CH4, H2O and their mixtures also including salt with the Excel macro "CO2Thermodynamics". SINTEF report 2014, Feb. 25.